Direct observation of self-energy signatures of the resonant collective mode in Bi_{2}Sr_{2}CaCu_{2}O_{8+δ}

Daixiang Mou, Adam Kaminski, and Genda Gu

Phys. Rev. B **95**, 174501 — Published 1 May 2017

DOI: 10.1103/PhysRevB.95.174501

Direct observation of self energy signatures of the resonant collective mode in $Bi_2Sr_2CaCu_2O_{8+\delta}$

Daixiang Mou and Adam Kaminski*
Division of Materials Science and Engineering, Ames Laboratory, Ames, Iowa 50011, USA
Department of Physics and Astronomy, Iowa State University, Ames, Iowa 50011, USA

Genda Gu
Condensed Matter Physics and Materials Science Department, Brookhaven National Laboratory, Upton, New York 11973, USA

We use high resolution ARPES to study the resonant, collective excitation mode in the superconducting state of Bi2212. By collecting very high quality data we found new features in the self energy in the antinodal region, where the interaction of electrons with the mode is the strongest. This interaction leads to pronounced peak in the scattering rate and we demonstrate that this feature is directly responsible for well known peak-dip-hump structure in cuprates. By studying how the weight of this peak changes with temperature we unequivocally demonstrate that interaction of electrons with resonant mode in cuprates vanishes at T_c and is very much localized in the momentum space close to the antinode. These findings present a consistent picture of line shape and self energy signatures of the electron-boson coupling in cuprates and resolve long standing controversy surrounding this issue. The momentum dependence of the strength of electron-mode interaction enables development of quantitative theory of this phenomenon in cuprates.

PACS numbers: 74.25.Jb, 74.72.Hs, 79.60.Bm

I. INTRODUCTION

In classical superconductors, the pairing and superconductivity is caused by interaction of electrons with phonons [1–3]. In unconventional superconductors such as cuprates [4, 5] or pnictides [6, 7], the origin of pairing is still debated, and a significant effort is made to identify the boson (if one exists) responsible for pairing. Several electron-boson interactions were discovered by ARPES in cuprates [8–21], however their role in the mechanism of the high temperature superconductivity remains unknown. The strongest of these interactions causes clearly visible features in the spectral line shape leading to famous "peak-dip-hump" structure [8–10, 22–25] and features in Raman spectra[26, 27]. This mode is attributed frequently to so called resonant mode first observed by inelastic neutron scattering [28–30], although some argued that this is a signature of very strong electron-phonon coupling [14, 18, 31, 32]. Some of the early papers advocating the phonon origin of this effect were based on seemingly isotropic behavior around the Fermi surface [14] and observation of isotope effect [31] at high binding energies. Other result clearly demonstrated that this interaction varies strongly with momentum and temperature and is strongest in the antinodal region, where the superconducting gap reaches maximum magnitude [12, 18, 32], although there were some arguments that phonons can also couple to electrons in highly anisotropic manner [18, 32]. The isotope effects studies so far still lack consensus [31, 33–35]. A theoretical model also proposed that electron-phonon interaction can indeed change abruptly across T_c [32], although this does not occur in classical superconductors [36].

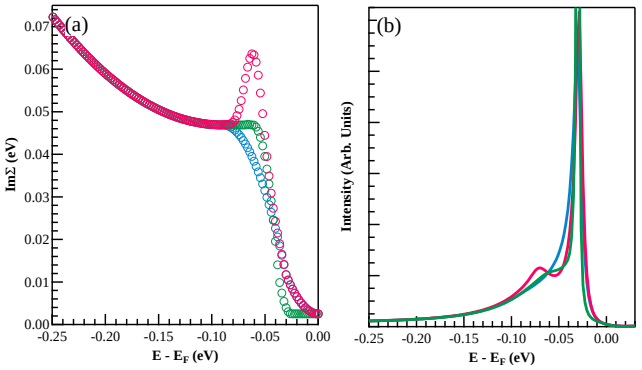

FIG. 1. (Color) EDC line shape simulation. (a) three different ImΣ models, two with a broadened step-like functions (blue and green circles) and one with a peak structure (red circle) at 60meV. (b) Simulated k_F EDCs in superconducting state. Gap size of 30 meV is used in all simulations. Detailed simulation procedure is described in Ref. [36].

Presence of a collective excitation in a material has pronounced effects on both real (ReΣ) and imaginary (ImΣ) part of the self energy [12, 37], a quantity that can be readily extracted from ARPES data [37]. Indeed, a significant progress was made in the nodal region of the momentum space using such approach [8, 9, 11–21]. The main obstacle in examining the detailed temperature dependence at the antinode is lack of objective measure of its strength due to rapid broadening of the peaks above T_c and the proximity of the band bottom to the chem-

* kaminski@ameslab.gov

ical potential at antinode. Here we solve this decades, longstanding problems by using double Lorentzian fits to ultra high quality and statistics data. This approach allowed us to successfully extract the self energy in the antinodal part of the Brillouin zone and resolve this important issue once and for all. We are not aware of other previous attempts to extract the ImΣ at the antinode. It is possible that requirement of very high data statistics was a barrier for experiments carried out at synchrotron due to time limits and sample aging [38]. We found very pronounced peak in the ImΣ in the close proximity of the antinode at energy expected based on the inelastic neutron scattering studies. Upon warming up, the amplitude of this peak decreases in order parameter-like fashion and it disappears completely above T_c. The temperature dependence of this feature follows exactly the intensity of the resonant mode reported by neutron measurements. The momentum dependence of this feature will provide new insights and guidance to theory to establish the relation of this effect to the high temperature superconductivity in cuprates.

II. EXPERIMENTAL DETAILS

Optimally doped single crystals of Bi2212 (T_c = 95 K) were grown by the conventional floating-zone technique and used in number of previous studies [39–41]. We note that the T* for these samples is around 230K, therefore substantially higher than T_c as demonstrated in Ref. [41]. The samples were cleaved *in situ* at base pressure lower than 5×10^{-11} Torr. The cleaved surface displayed no observable aging effects for duration of measurements as verified by temperature cycling. ARPES measurements were carried out using a laboratory-based system consisting of a Scienta SES2002 electron analyzer and GammaData Helium UV lamp equipped with custom designed refocusing optics. All data were acquired using the HeI line with a photon energy of 21.2 eV. The angular resolution was 0.13° and $\sim$ 0.5° along and perpendicular to the direction of the analyzer slits, respectively. The energy corresponding to the chemical potential was determined from the Fermi edge of a polycrystalline Au reference in electrical contact with the sample. The energy resolution was set at $\sim$6meV - confirmed by measuring the energy width between 90% and 10% of the Fermi edge from the same Au reference. The data were measured using several samples yielding consistent results.

ImΣ is obtained by fitting the Momentum Distribution Curve (MDC) with Lorenzians [12, 37]. The half width of Lorenz peak (Δk) is proportional to ImΣ: $Im\Sigma = \Delta k \times \nu_0$, where ν_0 is the bare Fermi velocity. At the node this is a straight forward procedure as there is only a single, relatively sharp, highly dispersive band present. Close to the antinode such procedure becomes much more complicated because the bottom of the band is located close to the chemical potential and relatively broad peaks for positive and negative momentum partially overlap. To overcome these problems, we fitted the MDC data at each binding energy with two lorentzians. We took care verifying that the dispersion determined by the positions of these peaks agrees with the overall data. Such obtained dispersion data allows us also to determine the velocity that is necessary for calculating the ImΣ.

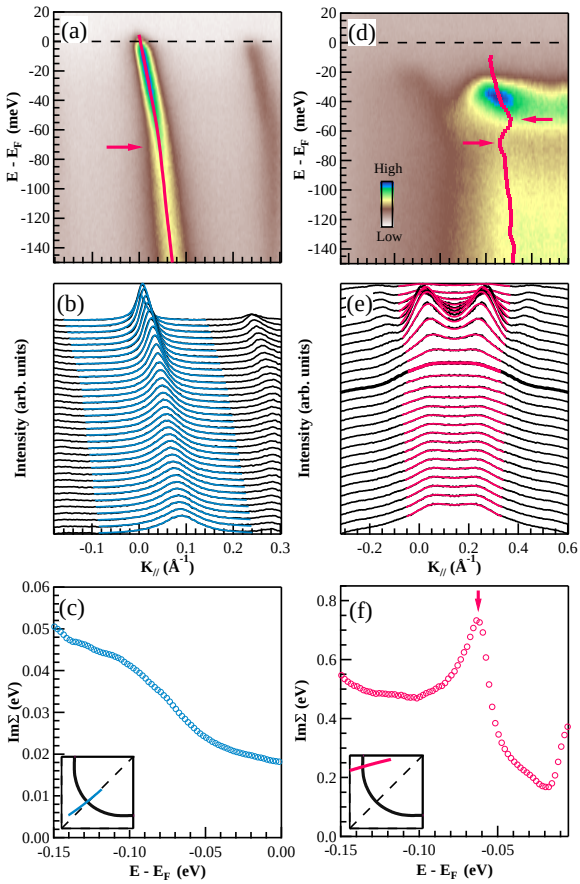

FIG. 2. (color) Typical MDC fitting results. (a) Measured spectra image along nodal cut at 16 K. Cut location is illustrated in the insert of (c). Obtained band dispersion is superimposed on the image (blue solid line). (b) Corresponding MDCs (black solid lines) and fitting results (blue solid lines). Data are shifted vertically for clarity. (c) Energy dependent ImΣ of the cut in (a). (d) - (f) Similar as (a) - (c) with cut near antinodal region, as illustrated in the insert of (f). The MDCs in (e) are symmetrized from left to right with the momentum of band bottom . Thick black line marks the MDC at the energy of peak position in (f).

The presence of the peak in the ImΣ is a necessary condition for the appearance of the peak-dip-hump structure that is a hallmark of the ARPES line shape in the superconducting state of cuprates. We demonstrate this in Fig. 1a, where we model an ImΣ that has an abrupt suppression (two examples with different slope) below the mode energy and one that has an additional peak at the same energy. We than calculate the EDC intensities using standard expression for the spectral function and ReΣ obtained by Kramers Kronig transformation of the

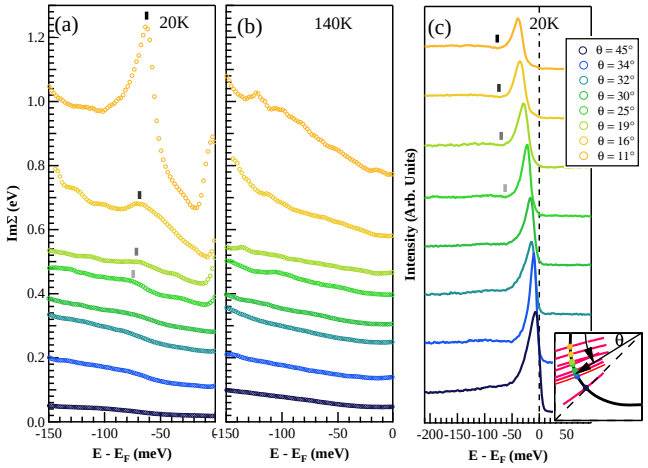

FIG. 3. (Color) Extracted energy dependent ImΣ along different cuts in Brillouin Zone at superconducting state 20 K (a) and normal state 140 K (b). Cut locations and θ definition are illustrated in right insert. Data are offset vertically with an 150 meV interval for each cut. (c) Extracted k_F EDCs from each cut measured at 20 K. Data are offset vertically for clarity. The black vertical bars in (a) and (c) mark the peak positions of ImΣ and the dip positions in EDC.

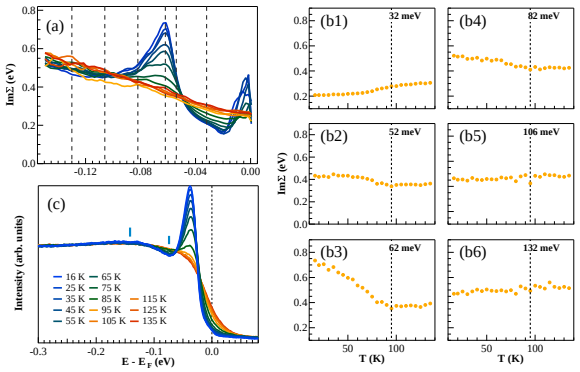

FIG. 4. (Color) Temperature dependent ImΣ of $\theta = 11°$ cut. (a) Energy dependent ImΣ at different temperatures. (b) Temperature dependent ImΣ at binding energy of 32 meV, 62 meV, 92 meV, 106 meV and 132 meV. Vertical doted line marks T_C. (c) k_F EDCs at different temperatures. The dip and hump positions are marked.

assumed ImΣ's. The results are shown in panel (b). In the first two cases, the resulting EDC has only a shoulder at the energy of the mode and no decrease of the intensity occurs. In the third case however, the presence of the peak in the ImΣ causes a clear dip, in qualitative agreement with hallmark EDC ARPES data lineshape. We therefore demonstrate that the presence of the dip in the EDC implies that the ImΣ must have a peak at similar energy.

III. RESULTS AND DISCUSSION

We now proceed to experimentally extract this information from our ultra high quality data. The key results along the node and antinode for T=16 K, well below T_c are shown in Fig. 2. In panels a, b and c we show the ARPES data along the node, fits to the MDCs and extracted ImΣ respectively. The nodal data and analysis are very similar to previous results demonstrating high degree of consistency. We observe several small bumps at high and low binding energies. Those most likely represent very weak coupling to ever-present phonons. Below, in panels d-f we present equivalent analysis of the data measured close to the antinode. The antinodal data is far more interesting, as such analysis was not carried out previously. The MDC's at high binding energy (bottom of panel e) are relatively broad, however it is clear that they consists of two separate peaks. At lower binding energies, the MDC marked as a bold line looks much more like a single broader peak and one can no longer easily distinguish two separate peaks. This is a clear signature that the line width of the two peaks that originate from the two branches for positive and negative momentum become broader than their separation at this binding energy and the overall MDC looks more like a single, broad peak. This agrees with the detailed results of extracted ImΣ shown in panel f. The ImΣ initially decreases with decreasing binding energy, then increases to nearly double of its initial value, reaching a peak at binding energy of 62 meV. At even lower energies, approaching the E_F, the ImΣ decrease rapidly to value well below one at high binding energies as expected. The upturn of the ImΣ near E_F is caused by superconducting gap opening.

We now move to study how this feature in ImΣ evolves with momentum by carrying out similar measurements and analysis along the entire Fermi surface. The results are summarized in Fig. 3. In the superconducting state (Fig. 3a), the previously mentioned peak structure can be clearly observed near antinode and is quite rapidly suppressed away from this part of the Brillouin zone with ImΣ evolving into a step-like structure around $\theta = 25°$ that remains to and is typical for the nodal direction. The energy position of the peak is shifting towards the higher binding energy as we move away from the antinode, indicating smooth variation of the mode energy coupled to electrons along Fermi surface. This evolution is consistent with the recent studies of the ReΣ using laser ARPES away from the antinodal region.[42, 43]. To contrast the behavior in the superconducting state, we show the extracted ImΣ along the same cuts in the normal state (140 K) in Fig. 3b. No obvious energy scale can be identified for any of these cuts signifying that these effects are somehow related to the superconducting state.

We now proceed to study in detail the temperature dependence of the self energy in the antinodal region. The extracted ImΣ for $\theta = 11°$ cut plotted as a function of temperature are shown in Fig. 4a. The peak in ImΣ is gradually suppressed with increasing temperature and

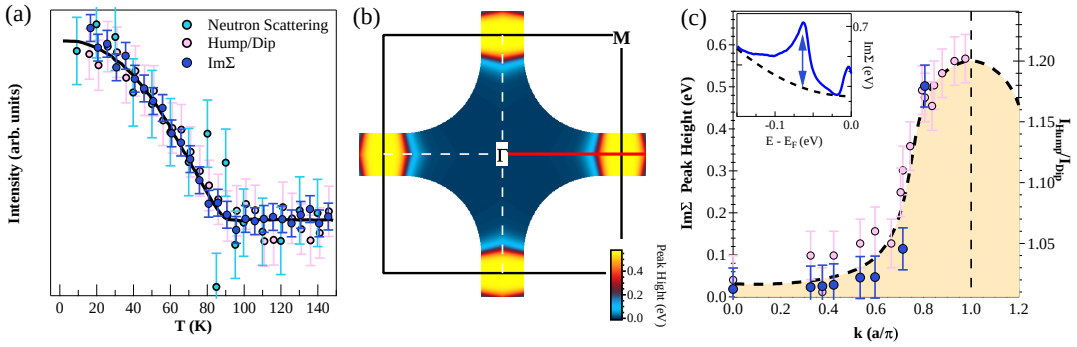

FIG. 5. (Color) (a) Temperature dependence of resonance mode intensity from neutron scattering (cyan solid circles)(Ref. [30]), ImΣ at 62 meV (blue solid circles) and dip to hump intensity ratio in k_F EDCs obtained from data in fig. 4c (pink solid circles). Data are shifted and normalized for comparison. The black line is a guide to the eye. (b) Momentum dependent peak height in ImΣ. (c) Peak height in ImΣ along Γ-X cut. As illustrated in the insert, peak hight height is obtained by subtracting a fitted ImΣ with formula $a\omega^2 + b$ (black dashed line in insert).

vanishes above T_c. We extract ImΣ at selected binding energies and plot them as a function of temperature in Fig. 4b. It is clear from these plots that the temperature dependence of the ImΣ changes qualitatively with binding energy. At low banding energies of 32 meV (slightly below the superconducting gap energy), the ImΣ is suppressed below T_c. This is consistent with earlier studies of the nodal region as one would expect equivalency between temperature and binding energy in the self energy. In contrast, at binding energy of 62 meV (peak position in ImΣ - see Fig. 4a), ImΣ begins to increase upon cooling just below T_c and then follows a BCS-like temperature dependence (panel b3). The increase of ImΣ upon cooling vanishes for higher binding energies as shown in panel b5 and b6 and the ImΣ does not display significant changes with temperature as expected.

We summarize the temperature and momentum dependence of the peak structure in ImΣ in Fig. 5. The comparison between ImΣ for binding energy of 62 meV and the ratio of the intensity at dip and hump energies are shown in Fig. 5a. Clearly they have the same temperature dependence that closely follows the intensity of the resonant peak measured in the inelastic neutron scattering experiments[30]. We stress that the T*∼230 K temperature for those samples is significantly higher than T_c[41], therefore the signatures of the resonant mode exist only in the superconducting state. In Fig. 5b we present a color plot of the peak value of the ImΣ throughout the Fermi surface. Fig. 5c shows how this quantity evolves along the Γ-X symmetry direction. The very high values of the ImΣ observed only in close proximity to the antinode, which is very consistent with the formation of the spin resonance mode in this region of momenta[30].

The discovery of the peak structure in ImΣ, together with its momentum and temperature dependence, provides a natural explanation of the peculiar spectra line shape observed in Bi2212 for more than two decades. Above T_c, in the antinodal region, EDC show a very broad peak, which is a hallmark of the normal state of optimally and underdoped cuprates. Upon cooling below T_c, a sharp quasiparticle peak forms at the energy corresponding to the superconducting gap and is followed by a dip then a hump at higher binding energies (Fig. 4c) [44]. The key proposal explaining the dip and hump structure relies on the interaction of electrons with a collective excitation [8, 9, 22, 44]. Such proposal necessarily requires existence of peak in the ImΣ. Our data provides definite evidence of its existence and the one to one correspondence between the peak in ImΣ and the dip-hump structure in EDC line shape validates those theory proposals. Our data reveals highly anisotropic momentum dependence of the enhancement of the ImΣ. This feature is almost completely extinguished within 20% of the M-Γ distance.

In summary, we describe a systematic investigation of the self energy in the antinodal region of optimally doped Bi2212. We find direct evidence of strong enhancement of the scattering rate in the superconducting state that manifests itself as a sharp peak in the ImΣ. We demonstrate that this feature is directly responsible for peak-dip-hump structure that attracted a lot of interest due to its intimate relation with superconductivity. The energy, temperature and momentum dependence of this feature matches very well with properties of the resonant mode reported by inelastic neutron scattering experiments. The observed peak in ImΣ vanishes around T=∼90K, which is similar to T_c for these samples and much lower than T* (=230K). This demonstrates that the resonant mode is linked with T_c rather than T*. The quantitative information about the momentum dependence of the strength of coupling to this collective excitation will provide guidance and validation of the theories explaining its detailed origin and relation to high temperature superconductivity.

We acknowledge very useful discussions with Mike Norman, Mohit Randeria, Nandini Trivedi, Andrey Chubukov and Joerg Schmalian. We are grateful to Takeshi Kondo for his experimental contributions. Re-

search was supported by the US Department of Energy, Office of Basic Energy Sciences, Division of Materials Sciences and Engineering. Ames Laboratory (ARPES measurements and data analysis) is operated for the US Department of Energy by the Iowa State University under Contract No. DE-AC02-07CH11358. Work at Brookhaven (sample growth) is supported by the Office of Basic Energy Sciences (BES), Materials Sciences and Engineering Division (MSED), U.S. Department of Energy (DOE) under Contract No. DE-SC0012704

[1] E. Maxwell, Phys. Rev. **78**, 477 (1950).
[2] C. A. Reynolds, B. Serin, W. H. Wright, and L. B. Nesbitt, Phys. Rev. **78**, 487 (1950).
[3] J. Bardeen, L. N. Cooper, and J. R. Schrieffer, Phys. Rev. **108**, 1175 (1957).
[4] A. Damascelli, Z. Hussain, and Z.-X. Shen, Rev. Mod. Phys. **75**, 473 (2003).
[5] J. Campuzano, M. Norman, and M. Randeria, in The Physics of Superconductors, edited by K. Bennemann and J. Ketterson (Springer Berlin Heidelberg, 2004) pp. 167–273–.
[6] D. C. Johnston, Advances in Physics **59**, 803 (2010).
[7] P. C. Canfield and S. L. Bud'ko, Annual Review of Condensed Matter Physics, Annu. Rev. Condens. Matter Phys. **1**, 27 (2010).
[8] Z.-X. Shen and J. R. Schrieffer, Phys. Rev. Lett. **78**, 1771 (1997).
[9] M. R. Norman, H. Ding, J. C. Campuzano, T. Takeuchi, M. Randeria, T. Yokoya, T. Takahashi, T. Mochiku, and K. Kadowaki, Phys. Rev. Lett. **79**, 3506 (1997).
[10] J. C. CAMPUZANO, H. Ding, M. R. Norman, H. M. Fretwell, M. Randeria, A. Kaminski, J. Mesot, T. Takeuchi, T. Sato, T. Yokoya, T. Takahashi, T. Mochiku, K. Kadowaki, P. Guptasarma, D. G. Hinks, Z. Konstantinovic, Z. Z. Li, and H. Raffy, Phys. Rev. Lett. **83**, 3709 (1999).
[11] P. V. Bogdanov, A. Lanzara, S. A. Kellar, X. J. Zhou, E. D. Lu, W. J. Zheng, G. Gu, J.-I. Shimoyama, K. Kishio, H. Ikeda, R. Yoshizaki, Z. Hussain, and Z. X. Shen, Phys. Rev. Lett. **85**, 2581 (2000).
[12] A. Kaminski, M. Randeria, J. C. Campuzano, M. R. Norman, H. Fretwell, J. Mesot, T. Sato, T. Takahashi, and K. Kadowaki, Phys. Rev. Lett. **86**, 1070 (2001).
[13] P. D. Johnson, T. Valla, A. V. Fedorov, Z. Yusof, B. O. Wells, Q. Li, A. R. Moodenbaugh, G. D. Gu, N. Koshizuka, C. Kendziora, S. Jian, and D. G. Hinks, Phys. Rev. Lett. **87**, 177007 (2001).
[14] A. Lanzara, P. V. Bogdanov, X. J. Zhou, S. A. Kellar, D. L. Feng, E. D. Lu, T. Yoshida, H. Eisaki, A. Fujimori, K. Kishio, J.-I. Shimoyama, T. Noda, S. Uchida, Z. Hussain, and Z.-X. Shen, Nature **412**, 510 (2001).
[15] X. J. Zhou, T. Yoshida, A. Lanzara, P. V. Bogdanov, S. A. Kellar, K. M. Shen, W. L. Yang, F. Ronning, T. Sasagawa, T. Kakeshita, T. Noda, H. Eisaki, S. Uchida, C. T. Lin, F. Zhou, J. W. Xiong, W. X. Ti, Z. X. Zhao, A. Fujimori, Z. Hussain, and Z.-X. Shen, Nature **423**, 398 (2003).
[16] T. Sato, H. Matsui, T. Takahashi, H. Ding, H.-B. Yang, S.-C. Wang, T. Fujii, T. Watanabe, A. Matsuda, T. Terashima, and K. Kadowaki, Phys. Rev. Lett. **91**, 157003 (2003).
[17] S. V. Borisenko, A. A. Kordyuk, T. K. Kim, A. Koitzsch, M. Knupfer, J. Fink, M. S. Golden, M. Eschrig, H. Berger, and R. Follath, Phys. Rev. Lett. **90**, 207001 (2003).
[18] T. Cuk, F. Baumberger, D. H. Lu, N. Ingle, X. J. Zhou, H. Eisaki, N. Kaneko, Z. Hussain, T. P. Devereaux, N. Nagaosa, and Z.-X. Shen, Phys. Rev. Lett. **93**, 117003 (2004).
[19] A. A. Kordyuk, S. V. Borisenko, V. B. Zabolotnyy, J. Geck, M. Knupfer, J. Fink, B. Büchner, C. T. Lin, B. Keimer, H. Berger, A. V. Pan, S. Komiya, and Y. Ando, Phys. Rev. Lett. **97**, 017002 (2006).
[20] W. S. Lee, K. Tanaka, I. M. Vishik, D. H. Lu, R. G. Moore, H. Eisaki, A. Iyo, T. P. Devereaux, and Z. X. Shen, Phys. Rev. Lett. **103**, 067003 (2009).
[21] T. Kondo, Y. Nakashima, W. Malaeb, Y. Ishida, Y. Hamaya, T. Takeuchi, and S. Shin, Phys. Rev. Lett. **110**, 217006 (2013).
[22] M. R. Norman and H. Ding, Phys. Rev. B **57**, R11089 (1998).
[23] R. Zeyher and A. Greco, Phys. Rev. B **64**, 140510 (2001).
[24] M. Eschrig and M. R. Norman, Phys. Rev. B **67**, 144503 (2003).
[25] M. Eschrig, Advances in Physics **55**, 47 (2006).
[26] R. Zeyher and A. Greco, Phys. Rev. B **87**, 224511 (2013).
[27] B. Loret, S. Sakai, S. Benhabib, Y. Gallais, M. Cazayous, M. A. Measson, R. D. Zhong, J. Schneeloch, G. D. Gu, A. Forget, D. Colson, I. Paul, M. Civelli, and A. Sacuto, arXiv:1703.00794 (2017).
[28] J. Rossat-Mignod, L. Regnault, C. Vettier, P. Bourges, P. Burlet, J. Bossy, J. Henry, and G. Lapertot, Physica C: Superconductivity **185-189, Part 1**, 86 (1991).
[29] H. A. Mook, M. Yethiraj, G. Aeppli, T. E. Mason, and T. Armstrong, Phys. Rev. Lett. **70**, 3490 (1993).
[30] H. F. Fong, P. Bourges, Y. Sidis, L. P. Regnault, A. Ivanov, G. D. Gu, N. Koshizuka, and B. Keimer, Nature **398**, 588 (1999).
[31] G.-H. Gweon, T. Sasagawa, S. Zhou, J. Graf, H. Takagi, D.-H. Lee, and A. Lanzara, Nature **430**, 187 (2004).
[32] T. P. Devereaux, T. Cuk, Z.-X. Shen, and N. Nagaosa, Phys. Rev. Lett. **93**, 117004 (2004).
[33] J. F. Douglas, H. Iwasawa, Z. Sun, A. V. Fedorov, M. Ishikado, T. Saitoh, H. Eisaki, H. Bando, T. Iwase, A. Ino, M. Arita, K. Shimada, H. Namatame, M. Taniguchi, T. Masui, S. Tajima, K. Fujita, S.-i. Uchida, Y. Aiura, and D. S. Dessau, Nature **446**, E5 (2007).
[34] H. Iwasawa, Y. Aiura, T. Saitoh, H. Eisaki, H. Bando, A. Ino, M. Arita, K. Shimada, H. Namatame, M. Taniguchi, T. Masui, S. Tajima, M. Ishikado, K. Fujita, S. Uchida, J. Douglas, Z. Sun, and D. Dessau, Physica C: Superconductivity and its Applications **463-465**, 52 (2007).
[35] H. Iwasawa, J. F. Douglas, K. Sato, T. Masui, Y. Yoshida, Z. Sun, H. Eisaki, H. Bando, A. Ino, M. Arita, K. Shimada, H. Namatame, M. Taniguchi, S. Tajima, S. Uchida, T. Saitoh, D. S. Dessau, and

Y. Aiura, Phys. Rev. Lett. **101**, 157005 (2008).
[36] D. Mou, R. Jiang, V. Taufour, R. Flint, S. L. Bud'ko, P. C. Canfield, J. S. Wen, Z. J. Xu, G. Gu, and A. Kaminski, Phys. Rev. B **91**, 140502 (2015).
[37] T. Valla, A. V. Fedorov, P. D. Johnson, and S. L. Hulbert, Phys. Rev. Lett. **83**, 2085 (1999).
[38] A. D. Palczewski, T. Kondo, J. S. Wen, G. Z. J. Xu, G. Gu, and A. Kaminski, Phys. Rev. B **81**, 104521 (2010).
[39] T. Kondo, R. Khasanov, T. Takeuchi, J. Schmalian, and A. Kaminski, Nature **457**, 296 (2009).
[40] T. Kondo, Y. Hamaya, A. D. Palczewski, T. Takeuchi, J. S. Wen, Z. J. Xu, G. Gu, J. Schmalian, and A. Kaminski, Nat Phys **7**, 21 (2011).
[41] T. Kondo, A. D. Palczewski, Y. Hamaya, T. Takeuchi, J. S. Wen, Z. J. Xu, G. Gu, and A. Kaminski, Phys. Rev. Lett. **111**, 157003 (2013).
[42] J. He, W. Zhang, J. M. Bok, D. Mou, L. Zhao, Y. Peng, S. He, G. Liu, X. Dong, J. Zhang, J. S. Wen, Z. J. Xu, G. D. Gu, X. Wang, Q. Peng, Z. Wang, S. Zhang, F. Yang, C. Chen, Z. Xu, H.-Y. Choi, C. M. Varma, and X. J. Zhou, Phys. Rev. Lett. **111**, 107005 (2013).
[43] N. C. Plumb, T. J. Reber, H. Iwasawa, Y. Cao, M. Arita, K. Shimada, H. Namatame, M. Taniguchi, Y. Yoshida, H. Eisaki, Y. Aiura, and D. S. Dessau, New Journal of Physics **15**, 113004 (2013).
[44] D. S. Dessau, B. O. Wells, Z.-X. Shen, W. E. Spicer, A. J. Arko, R. S. List, D. B. Mitzi, and A. Kapitulnik, Phys. Rev. Lett. **66**, 2160 (1991).